

Risk-Aware Autonomous Driving for Linear Temporal Logic Specifications

Shuhao Qi¹, Zengjie Zhang¹, Zhiyong Sun² and Sofie Haesaert¹

Abstract—Decision-making for autonomous driving incorporating different types of risks is a challenging topic. This paper proposes a novel risk metric to facilitate the driving task specified by linear temporal logic (LTL) by balancing the risk brought up by different uncertain events. Such a balance is achieved by discounting the costs of these uncertain events according to their timing and severity, thereby reflecting a human-like awareness of risk. We have established a connection between this risk metric and the occupation measure, a fundamental concept in stochastic reachability problems, such that a risk-aware control synthesis problem under LTL specifications is formulated for autonomous vehicles using occupation measures. As a result, the synthesized policy achieves balanced decisions across different types of risks with associated costs, showcasing advantageous versatility and generalizability. The effectiveness and scalability of the proposed approach are validated by three typical traffic scenarios in Carla simulator.

I. INTRODUCTION

Developing motion-planning frameworks for autonomous vehicles remains a significant challenge due to the inherent complexity and uncertainty of real-world traffic scenarios [1], [2]. The complexity primarily arises from the diverse and comprehensive concerns in a practical driving task, including safety [3], traffic rules [4], and social norms [5], [6]. The uncertainty mainly originates from the dynamic environment with unpredictable traffic participants [7] and unexpected events [8]. Taking an unprotected turn scenario [9] in Fig. 1 as an example, the ego vehicle must take a left turn to reach a predefined goal without collisions with the opponent car. It must obey the traffic rules by correctly reacting to the traffic light, rendering a motion planning problem subject to hard spatiotemporal constraints [10]. Moreover, it should also follow certain driving norms, such as giving priority to an opponent car driving from the opposite direction. The environmental uncertainty brings additional challenges to the driving task by imposing the ego vehicle to the potential risk of violating the specifications above, even rendering the task infeasible in extreme cases [11]. A risk-aware autonomous driving scheme requires the ego vehicle to make decisions incorporating different risks associated with safety, traffic rules, and social norms, as mentioned above.

Temporal logic provides a formal and expressive framework to describe high-level tasks that incorporates both spatial and temporal constraints [12], [13] and synthesize



Fig. 1: Unprotected turn in an intersection

provably correct controllers [14], making itself well-suited to encode traffic tasks with rules and norms [15] and enhance trustworthiness in motion planning tasks [16], [17]. For motion planning in an uncertain environment, risk can be quantified as the probability that a temporal logic specification fails [18]. To develop a risk-aware control policy, many control synthesis problems focus on maximizing the satisfaction probability of temporal logic specifications, i.e., minimizing the violation risk [19]–[21]. However, such risk metrics are not suitable for realistic traffic where different types of risky events may be involved [22]. In this sense, a rational policy should prioritize events according to their emergency and timing [23]. For example, the dangers in the near future should be prioritized compared to those in the far future [24]. Unfortunately, a single satisfaction probability of temporal logic specifications in most previous methods cannot differentiate the severity and timing of events [25], potentially resulting in unsafe driving behavior. Thus, a novel risk-aware motion planning method is needed to balance different types of risk according to the severity and timing of various events [26], ensuring more reliable and human-like decision-making in traffic scenarios [27].

A model commonly used in the transportation field, named driver’s risk field [24], [28], has been designed to mimic a human-like awareness of risk by incorporating discounting factors and cost functions for different events [29]. We believe similar techniques can also be used to address the above limitations of satisfaction probability of temporal logic. Notably, we found the connection between the risk field model and the occupation measure, a key concept for solving a stochastic reachability problem for a Markov Decision Process (MDP) [30]. The occupation measure has been used as heuristics to guide an efficient search for motion planning problems [31]. In [32], it is used to synthesize

This work was supported by the European project SymAware under the grant No. 101070802, and by the European project COVER under the grant No. 101086228.

¹ S. Qi, Z. Zhang, S. Haesaert are with the Department of Electrical Engineering, Eindhoven University of Technology, Eindhoven, The Netherlands. {s.qi, z.zhang3, s.haesaert}@tue.nl

² Z. Sun is with the College of Engineering, Peking University, Beijing, China. {zhiyong.sun@pku.edu.cn}

policies that balance different probabilities of temporal logic specifications for Markov decision process (MDP) models by a coupled linear programming (LP) problem, providing an efficient solution for control synthesis with balanced risk. In [33], it has been used to derive a robust control policy with probabilistic guarantees, addressing a correct-by-design solution for systems with stochastic uncertainty. Inspired by this, we propose to incorporate the risk field model into the control synthesis problem using occupation measures.

This paper proposes a novel risk-aware motion planning framework for autonomous vehicles incorporating different types of risk in a dynamic and uncertain environment. Firstly, we employ a combination of safety and co-safety specifications, which are LTL fragments [34], to represent traffic tasks without losing expressivity. Such specifications allows to convert the control synthesis problem into a reachability problem, which avoid expensive computations. Secondly, we develop a novel risk metric for LTL specifications, which accounts for the timing and severity of different uncertain events. In addition, we establish the connection between this risk metric and the occupation measure dedicated to a reachability problem. Finally, a stochastic reachability problem subject to this risk metric is formulated as an LP problem to synthesize risk-aware driving policy. Such a policy can balance different types of risks, including the collision risk and the violation risk of traffic rules and norms, in terms of their timing and severity. The effectiveness and scalability of the proposed method are validated in three distinct driving scenarios using the high-fidelity Carla simulator [35], demonstrating its capability to handle complexities from traffic rules and unexpected events due to uncertainty, and its scalability across versatile scenarios.

II. PRELIMINARY AND PROBLEM STATEMENT

A. Finite-State Model for Vehicles and Environments

MDP is a mathematical framework for decision-making in stochastic environments. Hence, a finite-state MDP is leveraged to capture the uncertain behavior of vehicles.

Definition 1. A Markov decision process (MDP) is a tuple $\mathcal{M} = (S, s_0, A, \mathbb{T})$ with S is a finite set of states and $s_0 \in S$ is an initial state; A is a finite set of actions; and $\mathbb{T}: S \times A \times S \rightarrow [0, 1]$ is a probabilistic transition kernel. \square

We denote a finite path of \mathcal{M} as $\mathbf{s}_n := s_0 a_0, \dots, s_{n-1} a_{n-1} s_n, n \in \mathbb{N}$, with $s_i \in S$ and $a_i \in A$, for all $i \leq n$. Similarly, we denote an infinite paths as $\mathbf{s} = s_0 a_0 s_1 a_1 \dots$. The inputs of \mathcal{M} are selected according to a policy defined as follows.

Definition 2. A policy is a sequence $\pi = \pi_0 \pi_1 \pi_2 \dots$ of stochastic kernels $\pi_n: H \times A \rightarrow [0, 1]$, where H denotes the collection of all the finite paths \mathbf{s}_n . The set of all policies is denoted by Π .

Given a policy $\pi \in \Pi$ and a finite path \mathbf{s}_n , the distribution of the next control input a_n is given by $\pi_n(\cdot | \mathbf{s}_n)$ with $\sum_{a_n} \pi_n(a_n | \mathbf{s}_n) = 1$. Given the initial state s_0 , the stochastic kernel $s_{n+1} \sim \mathbb{T}(\cdot | s_n, a_n)$ together with the policy

$a_n \sim \pi_n(\cdot | \mathbf{s}_n)$ induce a unique probability distribution over the paths of \mathcal{M} , which we denote by \mathbb{P}_π . Policies that depend on \mathbf{s}_n only through the current state s_n are called *Markov policies*, which means $\pi_n: S \times A \rightarrow [0, 1]$. A Markov policy is called stationary if the kernels π_n do not depend on the time index n . When it is applied to the MDP, the resulting model is called a Markov Chain (MC), defined as follows,

Definition 3. A Markov Chain (MC) is defined as a tuple $\mathcal{C} = (S, s_0, \mathbb{T})$ where S and s_0 are defined as in the MDP, and $\mathbb{T}: S \times S \rightarrow [0, 1]$ is a probabilistic transition kernel. \square

Since the environmental states are uncontrollable, it is proper to use an MC model to represent the evolution of environments [36]. To sum up, an MDP model denoted by $\mathcal{M}_v = (S_v, s_{v,0}, A, \mathbb{T}_v)$ is used to represent the behavior of the ego vehicle, and an MC model denoted by $\mathcal{C}_e = (S_e, s_{e,0}, \mathbb{T}_e)$ to capture the behavior of the environment. Furthermore, The composition of \mathcal{M}_v and \mathcal{C}_e is also an MDP model, defined as $\bar{\mathcal{M}} = (\bar{S}, \bar{s}_0, A, \bar{\mathbb{T}})$, where $\bar{S} := S_v \times S_e$, $\bar{s}_0 = (s_{v,0}, s_{e,0})$, and $\bar{\mathbb{T}}: \bar{S} \times A \times \bar{S} \rightarrow [0, 1]$ based on $\bar{\mathbb{T}}(\bar{s}, a, \bar{s}') = \mathbb{T}_v(s_v, a, s'_v) \times \mathbb{T}_e(s_e, s'_e)$.

B. Specifications: Linear Temporal Logic (LTL)

The set of atomic propositions $\text{AP} = \{p_1, \dots, p_N\}$ defines an alphabet $\Sigma := 2^{\text{AP}}$, where each letter $\omega \in \Sigma$ contains the set of atomic propositions that are true. A labeling function \mathcal{L} maps states to letters in the alphabet Σ , such that an infinite path $\mathbf{s} = s_0 s_1 s_2 \dots$ generates a word as $\omega := \mathcal{L}(s_0) \mathcal{L}(s_1) \mathcal{L}(s_2) \dots$. A suffix of a word ω is $\omega_k = \omega_k \omega_{k+1} \omega_{k+2} \dots$, where $\omega_i \in \Sigma$ and $k \in \mathbb{N}_{\geq 0}$.

Syntax: An LTL [12] specification is recursively defined as,

$$\psi ::= \top \mid p \mid \neg\psi \mid \psi_1 \wedge \psi_2 \mid \bigcirc\psi \mid \psi_1 \text{U} \psi_2, \quad (1)$$

where ψ_1, ψ_2 and ψ are LTL formulas, $p \in \text{AP}$ is an atomic proposition, \neg is the *negation* operator, \wedge is the *conjunction* operator that connects two LTL formulas, and \bigcirc and U represent the *next* and *until* temporal operators, respectively. Other logical and temporal operators, namely *disjunction* \vee , *implication* \rightarrow , *eventually* \diamond , and *always* \square can be defined as, $\psi_1 \vee \psi_2 := \neg(\psi_1 \wedge \neg\psi_2)$, $\psi_1 \rightarrow \psi_2 := \neg\psi_1 \vee \psi_2$, $\diamond\psi := \top \text{U} \psi$, and $\square\psi := \neg\diamond\neg\psi$.

Semantics: For a given word ω , basic semantics of LTL are given as $\omega_k \models p$, if $p \in \omega_k$; $\omega_k \models \neg p$, if $p \notin \omega_k$; $\omega_k \models \psi_1 \wedge \psi_2$, if $\omega_k \models \psi_1$ and $\omega_k \models \psi_2$; $\omega_k \models \bigcirc\psi$, if $\omega_{k+1} \models \psi$; $\omega_k \models \psi_1 \text{U} \psi_2$, if $\exists i \in \mathbb{N}$ such that $\omega_{k+i} \models \psi_2$, and $\omega_{k+j} \models \psi_1$ holds $\forall 0 \leq j < i$.

Fragments: Two notable fragments of LTL are the safety and co-safety temporal logic fragments [34], which allows reasoning about the satisfaction of an infinite word using only a finite prefix. Specifically, a co-safety formula is satisfied if there exists a finite “good” prefix regardless of any infinite suffix. Conversely, the violation of a safety specification depends on the existence of a finite bad prefix. In other words, safety fragments represent “bad thing never happens”, while co-safety fragments depict “good thing eventually happens”. A syntactically co-safety LTL (scLTL) formula ψ

over a set of atomic propositions AP is recursively defined

$$\psi ::= \text{true} \mid p \mid \neg p \mid \psi_1 \wedge \psi_2 \mid \psi_1 \vee \psi_2 \mid \bigcirc \psi \mid \psi_1 \text{U} \psi_2$$

where ψ_1 , ψ_2 , and ψ are scLTL formulas, and $p \in \text{AP}$. An LTL formula, ψ , is a safety specification if and only if its negation $\neg\psi$ is a co-safety specification.

Automaton: A general LTL specification can be translated into a Büchi automaton [12] whose semantics are defined over infinite words. In contrast, scLTL and safety specification can be also translated into deterministic finite-state automata (DFA), defined as follows.

Definition 4. An DFA is a tuple $\mathcal{A} = (Q, q_0, \Sigma, \delta, F)$, where Q is a finite set of states and $q_0 \in Q$ is an initial state; Σ is a finite input alphabet; $\delta : Q \times \Sigma \rightarrow Q$ is a deterministic transition function; $F \subset Q$ is a set of final states. \square

Final states are sink states, i.e., a path entering it stays there forever. The final states in the DFA from a co-safety specification are accepting states, while the final states in the DFA of a safety specification are non-accepting.

Study Case: In an intersection scenario depicted in Fig. 1, the ego vehicle is expected to eventually reach a target area labeled “ t ”, avoid collisions with the other vehicle labeled “ v ”, refrain from entering non-drivable areas labeled “ n ”, and also wait for a green light event labeled “ g ” before entering the intersection area labeled “ i ”. In this scenario, the LTL specification is $\psi = \psi_{cs} \wedge \psi_s$ with a co-safety formula $\psi_{cs} = \diamond(t)$ and a safety formula $\psi_s = \square(\neg g \rightarrow \neg i) \wedge \square(\neg n \wedge \neg v)$, defined over $\text{AP} = [t, v, g, i]$. DFAs can be autonomously translated from ψ_s and ψ_{cs} using off-the-shelf toolboxes [37].

C. Risk-Aware Control Synthesis Problem

Since traffic rules are primarily concerned with the occurrence of good or bad events rather than repetitive behaviors, we believe that the combination of safety and co-safety fragments can effectively represent nearly all traffic tasks and rules while mitigating the computational demand of control synthesis. Thus, we consider an LTL specification in the form of $\psi = \psi_{cs} \wedge \psi_s$ defined over an atomic proposition set AP, composed with a safety formula ψ_s and a co-safety formula ψ_{cs} . The corresponding DFAs of ψ_{cs} and ψ_s are denoted by \mathcal{A}_{cs} and \mathcal{A}_s , respectively. To represent the uncertain behavior of both the environment and vehicle, we use a composed MDP $\overline{\mathcal{M}}$, as defined in Definition 1. This composed MDP combines an MDP model for an ego vehicle, \mathcal{M}_v defined in Def. 1, and an MC model for an uncontrollable environment, \mathcal{C}_e defined in Definition 3. The states of $\overline{\mathcal{M}}$ are labeled by \mathcal{L} to an alphabet set Σ , which can be used to verify the satisfaction of ψ . To handle the uncertainty in realistic traffic like a human driver, we aim to develop a human-like risk metric for ψ and then synthesize a stochastic policy $\pi \in \Pi$ that respects a human-like risk metric.

III. HUMAN-LIKE RISK METRIC

Risk metrics are often defined based on simple reach-avoid problems [38]. Therefore, we will start by rewriting the satisfaction problem for the given specifications as a reach-avoid problems over product MDP.

A. Product MDP and Reachability Problem

Definition 5. The product MDP of $\overline{\mathcal{M}}$, \mathcal{A}_{cs} and \mathcal{A}_s is defined as a tuple $\mathcal{P} = (Z, z_0, A, \hat{\mathbb{T}}, G, D)$, with the state set $Z := S \times Q_{cs} \times Q_s$, the action set A , and the initial state $z_0 = (\bar{s}_0, \delta_{cs}(q_{cs}^0, \mathcal{L}(\bar{s}_0)), \delta_s(q_s^0, \mathcal{L}(\bar{s}_0)))$. $\hat{\mathbb{T}} : Z \times A \times Z \rightarrow [0, 1]$ is the probabilistic transition kernel, which can specify a transition from state $z_n = (\bar{s}_n, q_s^n, q_{cs}^n)$ to $z_{n+1} = (\bar{s}_{n+1}, q_s^{n+1}, q_{cs}^{n+1})$ under action $a_n \in A$ based on $\bar{s}_{n+1} \sim \hat{\mathbb{T}}(\cdot \mid \bar{s}_n, a_n)$, $q_{cs}^{n+1} = \delta_{cs}(q_{cs}^n, \mathcal{L}(\bar{s}_{n+1}))$ and $q_s^{n+1} = \delta_s(q_s^n, \mathcal{L}(\bar{s}_{n+1}))$ for each $n \in \mathbb{N}$. Denote the accepting set for ψ_{cs} as $G := \bar{S} \times F_{cs}$, and the non-accepting set for ψ_s as $D := \bar{S} \times F_s$.

It is well known [12] that the satisfaction probability of co-safety specification equates to a reachability probability towards the accepting state set of the product automaton defined in Def. 5,

$$\mathbb{P}_\pi(\omega \models \psi_{cs}) = \overline{\mathbb{P}}_{\bar{\pi}}(\diamond G) = \mathbb{E}_{\bar{\pi}}[\sum_t^\infty \mathbf{1}(z_t \in G)], \quad (2)$$

where $\mathbf{1}(\cdot)$ is an indicator function, $\bar{\pi}$ is policy for \mathcal{P} , and $\overline{\mathbb{P}}_{\bar{\pi}}$ denotes the probability distribution over the paths of \mathcal{P} under $\bar{\pi}$. Note that $\bar{\pi}$ for \mathcal{P} that is a Markovian and stationary policy, which is converted from π for \mathcal{M}_v defined in Def. 2. Similarly, for every safety specification ψ_s , the violation probability equates to a reachability probability towards the non-accepting state set of \mathcal{P} ,

$$\mathbb{P}_\pi(\omega \not\models \psi_s) = \overline{\mathbb{P}}_{\bar{\pi}}(\diamond D) = \mathbb{E}_{\bar{\pi}}[\sum_t^\infty \mathbf{1}(z_t \in D)]. \quad (3)$$

B. Limitations of Event Probability

However, using satisfaction and violation probability defined in (2) and (3) to evaluate safety in realistic traffic might lead to unnatural behavior. The event probability in (2) and (3) means that each possible trace generated by π that drives \mathcal{P} to enter into final states in finite time gets weight 1 and all else gets weighted 0, which is displayed in Fig. 2. Such an approach embraces two points against the awareness way of human drivers: (1) It does not account for the timing of violations, which may cause the vehicle to react too early to dangers that happen in the distant future; (2) It fails to consider varying costs associated with various types of violations, preventing the vehicle from appropriately balancing the seriousness of various dangers. Thus, a risk metric reflecting human-like risk awareness is necessary.

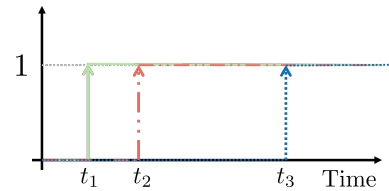


Fig. 2: Sketch for \mathbb{P}_π with three traces in different colors.

C. Using Discounting to Design Human-like Metrics

When rewards for decisions occur at different points in the future, discounted rewards are commonly used in reinforcement learning and economics. The discounted version

of satisfaction probability, $\mathbb{P}_\pi(\omega \models \psi_{cs})$, can be defined as,

$$\mathcal{V}_\pi = \mathbb{E}_\pi \left[\sum_t^\infty \gamma^t \mathbf{1}(z_t \in G) \right], \quad (4)$$

where $\gamma < 1$ is a discount factor. This discounting represents the preference of people for obtaining rewards sooner rather than later. The rationality of the discounting operation has also been supported by psychology studies [39]. When it comes to violation risks of safety specification, we propose a similar metric. In addition, varying costs of events are considered by a cost mapping function, denoted as $c(\cdot) : Z \rightarrow \mathbb{R}$, that assigns cost values to different product states. Specifically, $c(\hat{z}) = 0$ if $\hat{z} \notin D$, while $c(\hat{z}) > 0$ if $\hat{z} \in D$. Values of $c(\hat{z} \in D)$ is associated with ethical costs in real life. Furthermore, we propose the following metric to evaluate the risk of a policy π ,

$$\mathcal{R}_\pi = \mathbb{E}_\pi \left[\sum_t^\infty \gamma^t c(z_t) \right]. \quad (5)$$

The proposed metric can conquer the limitations of event probabilities. As depicted in Fig. 3, discounting reflects how a driver's awareness gradually decreases over time, causing the perceived risk for the same event to also diminish over time. When an event is significantly severe, like the one indicated by the red arrow, the risk metric in (5) will attach importance to this event more than less severe events. Therefore, this metric is able to consider the timing of events and also balance different severity of risks. In addition, this risk metric can be seen as a formalization of the concept of the driver's risk field (DRF) model [24], [28], which is widely used in the transportation field.

*The **Driver's Risk Field (DRF)** model is designed empirically to evaluate the uncertainty distribution from a driver's view. The risk field $\alpha(\cdot) : \mathbb{R}^2 \rightarrow \mathbb{R}$ maps horizontal coordinates to scalar values representing the driver's attention. To model human-like awareness, the DRF model operates on the intuition that the importance of future events diminishes while the corresponding uncertainty increases along the predictive horizon. The detailed formulation of DRF can be found in [24]. Subsequently, perceived risk can be evaluated via the expectation of the event cost, i.e., the product of the risk field and the cost map $c(\cdot) : \mathbb{R}^2 \rightarrow \mathbb{R}$ that represents the cost distribution over horizontal coordinates. Given a gridding discretization, the risk metric is defined as:*

$$\mathcal{R} = \sum_{x \in X} \sum_{y \in Y} c(x, y) \alpha(x, y), \quad (6)$$

where X and Y are finite sets consisting of discretized coordinates along with x and y -axis, respectively.

Inspired by the risk metric of DRF in Eq. (6), the risk metric in Eq. (5) can be rewritten as follows:

$$\begin{aligned} \mathcal{R}_\pi &= \mathbb{E}_\pi \left[\sum_t^\infty \sum_{z \in Z} \gamma^t c(z) \mathbf{1}(z_t = z) \right] \\ &= \sum_{z \in Z} c(z) \underbrace{\mathbb{E}_\pi \left[\sum_t^\infty \gamma^t \mathbf{1}(z_t = z) \right]}_{\beta_\pi(z)}. \end{aligned} \quad (7)$$

In this formulation, $\beta_\pi(z)$ is a discounted occupation measure. An occupation measure describes the expected amount

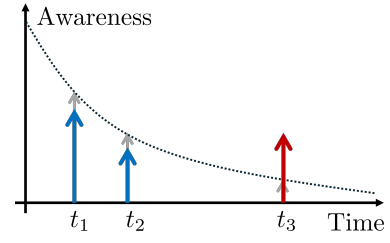


Fig. 3: Sketch for \mathcal{R}_π . The grey arrows indicate the awareness levels assigned to violation events, while the colored arrows represent the corresponding risk values. Red and blue colors differentiate between two different types of events.

of times that a state has been visited before reaching the final set given a Markov and stationary policy $\bar{\pi}(z, a)$, formulated as $\beta_\pi(z) := \mathbb{E}_\pi \left[\sum_{t=0}^\infty \mathbf{1}(z_t = z) \right]$. Occupation measures can be used to formulate stochastic shortest path problems [31]. By comparing risk metrics in (7) and (6), it is clear that the discounted occupation measure plays a similar role as the DRF model. In addition, the discounted occupation measure embraces similar awareness for events as the DRF model. Thus, we conjecture that the discounted occupation measure is equivalent to the human-like risk awareness model, DRF. Thus, we can integrate DRF into a control synthesis problem for LTL specification using discounted occupation measures.

IV. SYNTHESIS OF HUMAN-LIKE RISK-AWARE CONTROL

In this section, we formulate a reasonable control synthesis problem to trade off the rewards metric for co-safety specification and the risk metric for safety specification. A reasonable approach is to maximize the rewards metric and also keep the risk metric in an acceptable range, which is formulated as follows,

$$\max_{\bar{\pi}} \mathcal{V}_\pi(\omega \models \psi_{cs}) \quad \text{s.t.} \quad \mathcal{R}_\pi(\omega \models \psi_s) \leq r_{th}, \quad (8)$$

where $r_{th} \in \mathbb{R}$ is a constant threshold.

This problem can be formulated with discounted occupation measures defined over the product MDP, \mathcal{P} . Firstly, the discounted occupation measures with respect to product states, denoted by $\beta_\pi(z)$, equates to the sum of the discounted occupation measure with respect to state-action pairs, denoted by $\beta_\pi(z, a)$, over action set A , i.e., $\beta_\pi(z) = \sum_{a \in A} \beta_\pi(z, a)$. Specifically, $\beta_\pi(z, a)$ is defined as,

$$\beta_\pi(z, a) := \mathbb{E}_\pi \left[\sum_{t=0}^\infty \gamma^t \mathbf{1}(z_t = z, a_t = a) \right]. \quad (9)$$

For any $z' \in Z$, the occupation measure at state z' should satisfy the balance constraint to ensure the equivalence between the incoming transitions and the initial state distribution with the occupation measure at z' ,

$$\beta_\pi(z') = \sum_{z \in Z} \sum_{a \in A} \beta_\pi(z, a) \hat{\mathbb{T}}(z, a, z') + \mathbf{1}(z' = z_0), \quad (10)$$

A solution to this balance equation gives a stationary policy,

$$\bar{\pi}(z, a) = \frac{\beta_\pi(z, a)}{\sum_{a \in A} \beta_\pi(z, a)} = \frac{\beta_\pi(z, a)}{\beta_\pi(z)}. \quad (11)$$

For this policy, the reward metric for co-safety formula ψ_{cs} is formulated with discounted occupation measures as,

$$\bar{V}_{\bar{\pi}}(\diamond G) = \sum_{z' \in Z} \sum_{z \in Z} \sum_{a \in A} \beta_{\bar{\pi}}(z, a) \hat{\mathbb{T}}(z, a, z') + \mathbf{1}(z_0 \in G). \quad (12)$$

To sum up, the policy, reward metric, and risk metric are formulated with occupation measures in (11), (12) and (7). Therefore, the control synthesis problem in (8) can be formulated as a linear programming problem using $\beta_{\bar{\pi}}(z, a) \geq 0$ for all $(z, a) \in Z \times A$ as decision variables,

$$\begin{aligned} & \max_{\{\beta_{\bar{\pi}}(z, a)\}} \bar{V}_{\bar{\pi}}(\diamond G) \\ \text{s.t.} \quad & \sum_{z \in Z} \sum_{a \in A} c(z) \beta_{\bar{\pi}}(z, a) \leq r_{th} \\ & \beta_{\bar{\pi}}(z, a) \geq 0, \forall (z, a) \in Z \times A \\ & (10), \forall z' \in Z. \end{aligned} \quad (13)$$

This LP problem can be solved using an off-the-shelf solver, Gurobi [40]. If the problem is feasible, an optimal $\bar{\pi}$ can be extracted from the optimized occupation measures using Eq. (11), and then $\bar{\pi}$ can convert to $\pi \in \Pi$ defined on \mathcal{M}_v . The obtained policy is trustworthy since its risk metric is in the acceptable range. However, the LP problem may become infeasible sometimes. To address this, a relaxation variable can be introduced into the risk constraint. In practice, the relaxation variable can serve as an indicator of when a human driver should take over control of the vehicle.

V. IMPLEMENTATION AND EXPERIMENTAL STUDY

A. Implementation Framework

The above discussion is based on a MDP model of vehicles. However, to deploy this approach in a real car, we need to determine how to abstract an MDP model from vehicle systems and environments before formulating the proposed method, and how to implement the strategy based on abstract states after solving the LP problem. The complete framework for implementation on autonomous vehicles is illustrated in Fig. 4. More details can be found in the codes of a cute case [41].

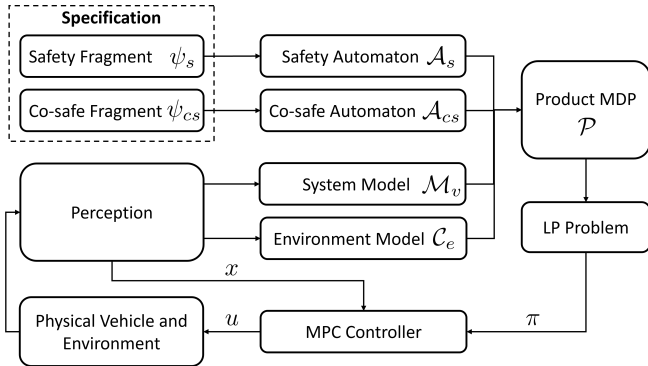


Fig. 4: The overall framework of control synthesis.

Vehicle dynamics: In the experiments, we consider the dynamics of vehicles with a discrete-time bicycle model. Specifically, the system state consists of the horizontal

position, heading angle, and linear speed of the vehicle, denoted by $[p_x, p_y]$, θ , and v , respectively. The control inputs to the vehicle are steering angle and acceleration, denoted by ϕ and a . Consequently, the system state is $\mathbf{x}(t) = [p_x(t), p_y(t), \theta(t), v(t)]^T \in \mathbb{X} \subset \mathbb{R}^4$, and the system input is $\mathbf{u}(t) = [\phi(t), a(t)]^T \in \mathbb{U} \subset \mathbb{R}^2$, where \mathbb{X} and \mathbb{U} are state space and input space, respectively. The kinematic model of the vehicle is a bicycle model $\mathbf{x}(t+1) = f(\mathbf{x}(t), \mathbf{u}(t))$ of which the details can be referred to in [42]. To capture the uncertainty of actuation and external factors, a zero-mean Gaussian-distributed disturbance vector, $\mathbf{w} \sim \mathcal{N}(0, \Sigma)$, is considered with the variance $\Sigma \in \mathbb{R}^{4 \times 4}$. The vehicle model with uncertainty is denoted by $\mathbf{x}_{k+1} = f(\mathbf{x}_k, \mathbf{u}_k) + \mathbf{w}(t)$.

From continuous dynamics to MDP: To abstract \mathcal{M}_v from the vehicle dynamics model with uncertainty, we first discretize the state space \mathbb{X} by gridding, where the finite state set S comprises the centers of the grid cells. For simplicity, this implementation considers only the horizontal positions of vehicles in \mathcal{M}_v . Similarly, the continuous input space \mathbb{U} is discretized into a finite action set A using appropriate interface functions. In this implementation, the transition probabilities are predefined by experts, which can also be generated autonomously and formally [21]. Additionally, AP is determined by corresponding propositions in specifications, and the labeling function \mathcal{L} can be extracted from the semantic maps in the perception module.

Control refinement: By solving the LP problem in Eq. (13), an optimal policy, π for \mathcal{M}_v , is obtained such that the next action be determined according to π . To track the reference state denoted by $\mathbf{x}_r \in \mathbb{X}$ corresponding to the next action, a model predictive controller (MPC) is designed to drive the dynamic model of vehicles, formulated as follows,

$$\begin{aligned} & \min_{\{\mathbf{u}_k\}_{k=0}^{N-1}} \sum_{k=0}^{N-1} (\mathbf{x}_{k+1} - \mathbf{x}_r)^T \mathbf{Q} (\mathbf{x}_{k+1} - \mathbf{x}_r) + \mathbf{u}_k^T \mathbf{R} \mathbf{u}_k \\ \text{s.t.} \quad & \mathbf{x}_{k+1} = f(\mathbf{x}_k, \mathbf{u}_k), \quad \mathbf{x}_0 = X_0, \\ & \mathbf{x}_{k+1} \in \mathbb{X}, \quad \mathbf{u}_k \in \mathbb{U}, \quad k=0, \dots, N-1, \end{aligned} \quad (14)$$

where N denotes a horizon number, X_0 is the current state, $\mathbf{Q} \in \mathbb{R}^{4 \times 4}$ and $\mathbf{R} \in \mathbb{R}^{2 \times 2}$ are diagonal weight matrixes. The first optimal control input \mathbf{u}_0 is deployed to the vehicle.

B. Risk Field Visualization

To visualize the risk field intuitively, we first consider a reach-avoid problem over the 2-dimensional positions of the ego vehicle, excluding the product states that include environment states and specification automaton states. Fig. 5 displays the risk field from discounted occupation measures obtained by solving the LP problem in Eq. (13). The red solid line represents the optimal path determined by the optimized risk field. As shown in the figure, we can see that the risk field obtained through the occupation measure aligns with the pattern of the proposed risk field in [24], which verifies the equivalence between the discounted occupation measure and DRF. In addition, the different risk thresholds r_{th} in Eq. (13) will change the shape of the risk field and the corresponding policy, implying different preference for predictive risks.

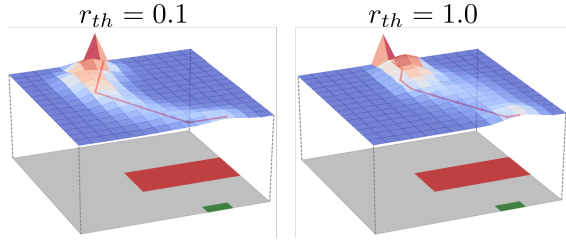


Fig. 5: Risk field extracted from discounted occupation measures. The higher layer is the risk field, while the lower layer is a map of a reach-avoid problem, where the red rectangle is an obstacle and the green rectangle is the target.

C. Simulation Results

We test the proposed method in three typical scenarios. The video demonstration of three scenarios is accessible at <https://youtu.be/0QMtpaREbHE>.

1) Unexpected construction scenario: Real-world traffic frequently encounters abnormal situations that make the original specifications infeasible [11], such as traffic participants violating rules or disruptions of traffic environments. We tested the proposed methods in such a scenario where an unexpected construction zone appears in the forward lane occupied by the ego vehicle, as illustrated in Fig. 6. In this case, the ego vehicle must deviate from a part of the original safety specifications to reach its target. The specification of this scenario for the ego vehicle is $\Box(\neg c \wedge \neg o \wedge \neg s) \wedge \Diamond(t)$, where c , o , s and t are labels for construction areas, opposite lanes, sidewalks, and target areas. We assign cost values of 10, 5, and 2 to the construction area, sidewalk, and opposite lane, respectively. The generated trajectory is shown in Fig. 6, where each blue rectangle represents the bounding box of the ego vehicle at a previous moment. We can see that the ego vehicle autonomously decides to bypass the construction zone via the opposite lane, which violates the safety specification but with the least violation, and finally reaches the target. This result shows that the proposed risk metric is helpful to yield trajectories that balance different risks and reduce violations as much as possible.

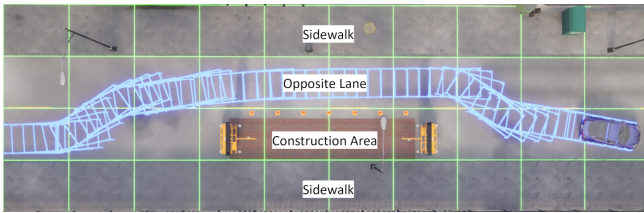


Fig. 6: The generated minimal-violation trajectory.

2) Pedestrian crossing scenario: In this scenario, we consider a dynamic environment where a pedestrian is crossing at a crosswalk. The ego vehicle is expected to respond appropriately to the pedestrian’s crossing behavior. To this end, we build an MC model to represent the process of pedestrian crossing behavior. The specification of the ego vehicle is $\Box(p \rightarrow \neg c) \wedge \Diamond(t)$, where c and t denote the crosswalk and target zone respectively, and p represents the presence of a pedestrian on the crosswalk. The ego

vehicle is expected to autonomously decide whether to stop or proceed based on the real-time situation. To test risk sensitivity, we set different risk thresholds r_{th} in the LP problem in Eq. (13). The simulation results, depicted in Fig. 7, indicate that the ego vehicle will stop at a smaller clearance ahead of the crosswalk as the increase of risk threshold, i.e., $r_{th} = 0.1, 1, 5$. But $r_{th} = 10$ is too high to make the ego car account for the collision risk such that the ego car directly hits the pedestrian, which is undesirable. This result demonstrates the parameter r_{th} can be used to tune the conservatism of the synthesized policy.

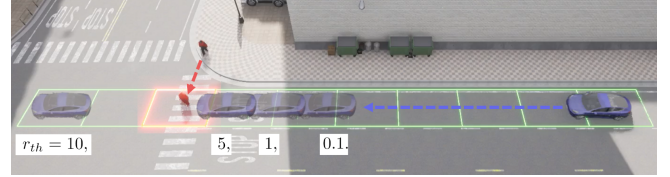


Fig. 7: Pedestrian crossing scenarios: transparent blue vehicles denote stopping points of different risk thresholds.

3) Unprotected turn scenario: We consider a complex intersection scenario that includes a traffic light system and dynamic opponent vehicles, as depicted in Fig. 1. The ego vehicle (blue car) is expected to follow traffic signals and avoid both non-drivable areas and the opponent vehicles (red car). The specification has been introduced in the study case of Sec. II-B. An MC model is designed to represent the switching of traffic lights and the movement of the opponent vehicle. For simplicity, We assume the opponent vehicle always moving forward. The collision risk with the opponent vehicle is calculated by calculating the overlap between risk fields of vehicles as the method used in [28]. The number of discounted occupation measures, i.e., decision variables of the formulated LP problem, is 2880. With the policy synthesized by the LP problem, the ego vehicle can wait at the boundary of the intersection until the light turns green and adjust its decisions based on the real-time positions of the opponent vehicles. Finally, the ego vehicle reaches the target position and successfully passes the intersection. The whole process is illustrated in Fig. 1 and the attached video, which validates the effectiveness of the proposed method. This case accounts for traffic lights, non-drivable areas, and other dynamic vehicles, which are typical factors in realistic traffic. Therefore, this method has the potential to scale to various scenarios and handle more complex situations.

VI. CONCLUSION

In this paper, we introduce a risk metric for temporal logic specifications using discounting, which can be connected to a typical human-like risk model. The proposed metric accounts for different types of risks in reality. The corresponding control synthesis problem can be solved using an efficient LP problem. Nevertheless, our current approach is still limited by not fully accounting for the interaction between the ego and other vehicles. Also, coarse discretization is introduced for computation efficiency. Future work will focus on addressing these limitations.

REFERENCES

- [1] N. Mehdipour, M. Althoff, R. D. Tebbens, and C. Belta, “Formal methods to comply with rules of the road in autonomous driving: State of the art and grand challenges,” *Automatica*, vol. 152, p. 110692, 2023.
- [2] W. Wang, L. Wang, C. Zhang, C. Liu, L. Sun, *et al.*, “Social interactions for autonomous driving: A review and perspectives,” *Foundations and Trends® in Robotics*, vol. 10, no. 3-4, pp. 198–376, 2022.
- [3] I. Hasuo, “Responsibility-sensitive safety: an introduction with an eye to logical foundations and formalization,” *arXiv preprint arXiv:2206.03418*, 2022.
- [4] S. Maierhofer, P. Moosbrugger, and M. Althoff, “Formalization of intersection traffic rules in temporal logic,” in *2022 IEEE Intelligent Vehicles Symposium (IV)*, pp. 1135–1144, IEEE, 2022.
- [5] I. Nastjuk, B. Herrenkind, M. Marrone, A. B. Brendel, and L. M. Kolbe, “What drives the acceptance of autonomous driving? an investigation of acceptance factors from an end-user’s perspective,” *Technological Forecasting and Social Change*, vol. 161, p. 120319, 2020.
- [6] F. Riaz, S. Jabbar, M. Sajid, M. Ahmad, K. Naseer, and N. Ali, “A collision avoidance scheme for autonomous vehicles inspired by human social norms,” *Computers & Electrical Engineering*, vol. 69, pp. 690–704, 2018.
- [7] J. Li, D. Isele, K. Lee, J. Park, K. Fujimura, and M. J. Kochenderfer, “Interactive autonomous navigation with internal state inference and interactivity estimation,” *IEEE Transactions on Robotics*, vol. 40, pp. 2932–2949, 2024.
- [8] T. Wongpiromsarn, K. Slutsky, E. Frazzoli, and U. Topcu, “Minimum-violation planning for autonomous systems: Theoretical and practical considerations,” in *2021 American Control Conference (ACC)*, pp. 4866–4872, IEEE, 2021.
- [9] Z. Shen, S. Li, Y. Liu, and X. Tang, “Analysis of driving behavior in unprotected left turns for autonomous vehicles using ensemble deep clustering,” *IEEE Transactions on Intelligent Vehicles*, pp. 1–13, 2023.
- [10] X. Meng and C. G. Cassandras, “Trajectory optimization of autonomous agents with spatio-temporal constraints,” *IEEE Transactions on Control of Network Systems*, vol. 7, no. 3, pp. 1571–1581, 2020.
- [11] J. Tůmová, L. I. Reyes Castro, S. Karaman, E. Frazzoli, and D. Rus, “Minimum-violation ltl planning with conflicting specifications,” in *2013 American Control Conference*, pp. 200–205, 2013.
- [12] C. Belta, B. Yordanov, and E. A. Gol, *Formal methods for discrete-time dynamical systems*, vol. 89. Springer, 2017.
- [13] L. Lindemann and D. V. Dimarogonas, “Control barrier functions for signal temporal logic tasks,” *IEEE control systems letters*, vol. 3, no. 1, pp. 96–101, 2018.
- [14] T. Wongpiromsarn, S. Karaman, and E. Frazzoli, “Synthesis of provably correct controllers for autonomous vehicles in urban environments,” in *2011 14th International IEEE Conference on Intelligent Transportation Systems (ITSC)*, pp. 1168–1173, IEEE, 2011.
- [15] S. Maierhofer, A.-K. Rettinger, E. C. Mayer, and M. Althoff, “Formalization of interstate traffic rules in temporal logic,” in *2020 IEEE Intelligent Vehicles Symposium (IV)*, pp. 752–759, IEEE, 2020.
- [16] C. Belta and S. Sadraddini, “Formal methods for control synthesis: An optimization perspective,” *Annual Review of Control, Robotics, and Autonomous Systems*, vol. 2, no. 1, pp. 115–140, 2019.
- [17] T. Wongpiromsarn, M. Ghasemi, M. Cubuktepe, G. Bakirtzis, S. Carr, M. O. Karabag, C. Neary, P. Gohari, and U. Topcu, “Formal methods for autonomous systems,” *arXiv preprint arXiv:2311.01258*, 2023.
- [18] L. Lindemann, N. Matni, and G. J. Pappas, “Stl robustness risk over discrete-time stochastic processes,” in *2021 60th IEEE Conference on Decision and Control (CDC)*, pp. 1329–1335, IEEE, 2021.
- [19] S. S. Farahani, R. Majumdar, V. S. Prabhhu, and S. Soudjani, “Shrinking horizon model predictive control with signal temporal logic constraints under stochastic disturbances,” *IEEE Transactions on Automatic Control*, vol. 64, no. 8, pp. 3324–3331, 2018.
- [20] S. Haesaert and S. Soudjani, “Robust dynamic programming for temporal logic control of stochastic systems,” *IEEE Transactions on Automatic Control*, vol. 66, no. 6, pp. 2496–2511, 2020.
- [21] B. C. van Huijgevoort, S. Weiland, and S. Haesaert, “Temporal logic control of nonlinear stochastic systems using a piecewise-affine abstraction,” *IEEE Control Systems Letters*, vol. 7, pp. 1039–1044, 2022.
- [22] L. Lindemann, G. J. Pappas, and D. V. Dimarogonas, “Reactive and risk-aware control for signal temporal logic,” *IEEE Transactions on Automatic Control*, vol. 67, no. 10, pp. 5262–5277, 2021.
- [23] M. Geisslinger, F. Poszler, J. Betz, C. Lütge, and M. Lienkamp, “Autonomous driving ethics: From trolley problem to ethics of risk,” *Philosophy & Technology*, vol. 34, no. 4, pp. 1033–1055, 2021.
- [24] S. Kolekar, J. de Winter, and D. Abbink, “Human-like driving behaviour emerges from a risk-based driver model,” *Nature Communications*, vol. 11, no. 1, p. 4850, 2020.
- [25] M. H. W. Engelaar, Z. Zhang, M. Lazar, and S. Haesaert, “Risk-aware mpc for stochastic systems with runtime temporal logics,” *arXiv preprint arXiv:2402.03165*, 2024.
- [26] W. M. D. Chia, S. L. Keoh, C. Goh, and C. Johnson, “Risk assessment methodologies for autonomous driving: A survey,” *IEEE transactions on intelligent transportation systems*, vol. 23, no. 10, pp. 16923–16939, 2022.
- [27] X. Li, “Trade-off between safety, mobility and stability in automated vehicle following control: An analytical method,” *Transportation research part B: methodological*, vol. 166, pp. 1–18, 2022.
- [28] Y.-J. Joo, E.-J. Kim, D.-K. Kim, and P. Y. Park, “A generalized driving risk assessment on high-speed highways using field theory,” *Analytic methods in accident research*, vol. 40, p. 100303, 2023.
- [29] M. Kwon, E. Biyik, A. Talati, K. Bhasin, D. P. Losey, and D. Sadigh, “When humans aren’t optimal: Robots that collaborate with risk-aware humans,” in *Proceedings of the 2020 ACM/IEEE international conference on human-robot interaction*, pp. 43–52, 2020.
- [30] E. Altman, “Constrained markov decision processes with total cost criteria: Occupation measures and primal lp,” *Mathematical methods of operations research*, vol. 43, no. 1, pp. 45–72, 1996.
- [31] F. Trevisan, S. Thiébaux, and P. Haslum, “Occupation measure heuristics for probabilistic planning,” in *Proceedings of the International Conference on Automated Planning and Scheduling*, vol. 27, pp. 306–315, 2017.
- [32] M. Guo and M. M. Zavlanos, “Probabilistic motion planning under temporal tasks and soft constraints,” *IEEE Transactions on Automatic Control*, vol. 63, no. 12, pp. 4051–4066, 2018.
- [33] S. Haesaert, P. Nilsson, and S. Soudjani, “Formal multi-objective synthesis of continuous-state mdps,” in *2021 American Control Conference (ACC)*, pp. 3428–3433, IEEE, 2021.
- [34] A. Artale, L. Geatti, N. Gigante, A. Mazzullo, and A. Montanari, “Complexity of safety and cosafety fragments of linear temporal logic,” in *Proceedings of the AAI Conference on Artificial Intelligence*, vol. 37, pp. 6236–6244, 2023.
- [35] A. Dosovitskiy, G. Ros, F. Codevilla, A. Lopez, and V. Koltun, “Carla: An open urban driving simulator,” in *Conference on robot learning*, pp. 1–16, PMLR, 2017.
- [36] A. Ulusoy, T. Wongpiromsarn, and C. Belta, “Incremental controller synthesis in probabilistic environments with temporal logic constraints,” *The International Journal of Robotics Research*, vol. 33, no. 8, pp. 1130–1144, 2014.
- [37] J. G. Henriksen, J. Jensen, M. Jørgensen, N. Klarlund, R. Paige, T. Rauhe, and A. Sandholm, “Mona: Monadic second-order logic in practice,” in *Tools and Algorithms for the Construction and Analysis of Systems: First International Workshop, TACAS’95 Aarhus, Denmark, May 19–20, 1995 Selected Papers 1*, pp. 89–110, Springer, 1995.
- [38] A. Majumdar and M. Pavone, “How should a robot assess risk? towards an axiomatic theory of risk in robotics,” in *Robotics Research: The 18th International Symposium ISRR*, pp. 75–84, Springer, 2020.
- [39] A. Ahmed, “Rationality and future discounting,” *Topoi*, vol. 39, no. 2, pp. 245–256, 2020.
- [40] Gurobi Optimization, LLC, “Gurobi Optimizer Reference Manual,” 2024.
- [41] S. Qi, “Ltl-formation-control,” *GitHub*, 2024. Available at https://github.com/Miracle-qi/Risk_LTL_Planning.
- [42] Z. Zhang, Z. Sun, and S. Haesaert, “Intention-aware control based on belief-space specifications and stochastic expansion,” *IEEE Transactions on Intelligent Vehicles*, 2024.